

SCIENTIFIC REPORTS



OPEN

Diffusion and distribution of deuterium in scandium deuteride thin films under irradiation of deuterium ion beam

Tao Wang^{1,2}, Jidong Long¹, Shiwei Wang³, Zhen Yang¹, Jie Li¹, Gang Huang¹, Linwen Zhang¹, Allen Jian Yang⁴ & Xiao Renshaw Wang^{4,5}

Scandium deuteride (ScD_x) thin films, as an alternative target for deuterium-deuterium (D-D) reaction, are a very important candidate for detection and diagnostic applications. Albeit with their superior thermal stability, the ignorance of the stability of ScD_x under irradiation of deuterium ion beam hinders the realization of their full potential. In this report, we characterize ScD_x thin films with scanning electron microscopy (SEM) and X-ray diffraction (XRD), Rutherford backscattering spectroscopy (RBS) and elastic recoil detection analysis (ERDA). We found with increased implantation of deuterium ions, accumulation and diffusion of deuterium are enhanced. Surprisingly, the concentration of deuterium restored to the value before implantation even at room temperature, revealing a self-healing process which is of great importance for the long-term operation of neutron generator.

Detection and diagnostic techniques employing neutron beams are extensively used for quality control in advanced manufacturing, contraband detection, advanced medicine, oil well logging, etc.¹⁻⁸. As an indispensable component of such kind of techniques, neutron generators take advantage of the deuterium-deuterium (D-D) reaction which generates a controllable high-flux neutron beam from a small source. This reaction is commonly triggered by bombarding a metal deuteride target with accelerated deuterium ions⁹. Thus the type and quality of the metal deuteride targets are of great importance to the D-D reaction. In the past two decades, various metal deuteride targets have been studied¹⁰⁻¹⁹. Nevertheless, they have a variety of shortcomings. For instance, titanium deuteride thin films, which are considered as the most promising target for D-D reaction, suffer from unsatisfactory thermal stability.

Scandium deuteride (ScD_x), as an alternative target for D-D reaction, has been drawing increasing attention because of its superior thermal stability¹⁷⁻²³. However, little is known about the content and distribution of deuterium in ScD_x thin films when they are subject to irradiation of deuterium ion beams although they are crucial to the stable operation of neutron generators. Herein, we report the characterization of ScD_x thin films under irradiation of deuterium ion beams, which reveals the accumulation of deuterium at the ion-implanted region and the subsequent rapid diffusion of deuterium at room temperature. We believe this reinstallation is a previously unknown self-healing process which is crucial to the stable operation of neutron generators based on D-D reaction.

Experimental Details

Preparation of ScD_x films. The molybdenum substrates were polished, rinsed with a mixed acid (nitric acid and sulfuric acid), washed in deionized water, cleaned in acetone ultrasonically for 30 min, and dried under a nitrogen atmosphere. The ScD_x thin films were grown by one-step reactive magnetron sputtering (Magnetron sputtering machine produced by Beijing Technol Science Co. Ltd). High purity argon gas (99.999%) and deuterium gas (99.999%) were used as the sputtering gas and reactive gas, respectively. A metallic Sc target of high

¹Institute of Fluid Physics, CAEP, P. O. Box 919-106, Mianyang, 621900, China. ²School of Nuclear Science and Technology, University of Science and Technology of China, Hefei, 230026, China. ³School of Sino-Russian, Heilongjiang University, Harbin, 150000, China. ⁴Division of Physics and Applied Physics, School of Physical and Mathematical Sciences, Nanyang Technological University, Singapore, 637371, Singapore. ⁵School of Electrical and Electronic Engineering, Nanyang Technological University, Singapore, 639798, Singapore. Correspondence and requests for materials should be addressed to T.W. (email: wangtaoxtc@gmail.com) or A.J.Y. (email: yangjian@ntu.edu.sg)

Sample number	Ion implanted	Energy	Ion current density	Dose
S1	/	/	/	/
S2	deuterium	120 keV	10 $\mu\text{A}/\text{cm}^2$	1*10 ¹⁷ atoms/cm ²
S3	deuterium	120 keV	10 $\mu\text{A}/\text{cm}^2$	5*10 ¹⁷ atoms/cm ²

Table 1. Parameters of irradiation experiments.

purity (99.95%) was utilized to deposit the ScD_x films^{24–26}. The base pressure was about 10^{−5} Pa. The total pressure of the (Ar + D₂) gas mixture was set at 0.4 Pa, while the rate of Ar flow and D₂ flow were 5 SCCM and 15 SCCM respectively. Two-micrometer-thick ScD_x thin films were deposited on Mo substrates at 573 K substrate temperature and −250 V DC substrate bias.

Irradiation experiment. The irradiation experiment was carried out with a multi-voltage accelerator. Deuterium ions produced by the ion source were accelerated with a voltage of 120 kV and implanted into the as-grown ScD_x thin films. Experimental parameters can be seen in the Table 1. Sample S1 is the as-grown sample, while samples S2 and S3 are irradiated by deuterium of different doses.

Characterization methods. A Phenom desktop G2 pro scanning electron microscope (SEM) was used to observe the surface morphology of the film surface. The X-ray diffraction (XRD) profiles were recorded using Cu K α radiation on X' Pert PRO that operated at 40 kV and 40 mA. The step size, angular range and counting time are $2\theta = 0.02^\circ$, $2\theta = 20\text{--}70^\circ$ and 1 second, respectively.

Elastic recoil detection analysis (ERDA) was employed to determine deuterium concentrations using the NEC 9SDH-2 \times 3 MV pelletron tandem accelerator at Fudan University. The chamber background pressure during ion beam analysis was lower than 1×10^{-4} Pa. The deuterium depth profiles in the samples were investigated by ERDA using a 4.5 MeV helium ion beam with a 75° incident angle with respect to the normal direction of the sample surface. A mylar foil with a thickness of 19 μm in front of the detector was used to absorb scattered helium. In addition, the composition of the film was determined by Rutherford Backscattering Spectroscopy (RBS) with 4.5 MeV helium ions beam perpendicular to the surface of the sample. The ERDA spectra were converted into deuterium concentration profiles by Alegria 1.0 code²⁷ with an expected systemic error below 7%. The atomic composition of the layer of the sample was given by RBS spectrum unfolding results analyzed with SIMNRA 6.03 code²⁸. Based on the RBS and ERDA measurements, we obtained the atomic ratio of D/Sc^{29–31}.

Results and Discussion

Figure 1 shows SEM images of the as-grown sample and implanted samples, demonstrating the microscopic irregularities on the surface. However, there is no observable morphological difference between the as-grown and irradiated samples, suggesting little mechanical damage due to the ion implantation.

Figure 2 shows the XRD patterns of the scandium deuteride thin films with and without deuterium ion irradiation. The structural analysis mainly indicates that the film has ScD₂ phase and substrate Mo phase. The intensities of ScD₂ phase peaks remain constant but the positions of these peaks shift to a smaller angle for the irradiated samples. It means that the lattice constants of scandium deuteride films increase after deuterium irradiation. No Sc phase peak is observed, suggesting that deuterium did not desorb from scandium deuteride film because the samples are water-cooled to prevent temperature rise.

A typical energy spectrum of He⁺ particles scattered from ScD_x/Mo film during irradiation of 4.5 MeV He⁺ with 0° incident angle is presented in the Fig. 3. The horizontal axis corresponds to the energy of the scattered He⁺, namely the depth from the specimen surface to the bulk. The energy spectrum profile reflects the structure of the layered ScD_x/Mo thin film, and thickness of the film. Apart from the Mo substrate and the top ScD_x thin film, no other elements are detected, proving the high purity of the grown ScD_x thin film.

The deuterium concentrations (atomic ratio of D to Sc) of scandium deuteride films, as shown in Fig. 4, were calculated from the standard analyses of ERD and RBS spectra. The lower horizontal axis corresponds to the areal density of scandium deuteride film, namely the distance from the sample surface to the bulk (about 2 μm), which is indicated by the upper horizontal axis. The vertical axis corresponds to the deuterium concentration in the scandium deuteride film. The average D/Sc atomic ratio is 1.74 ± 0.08 .

After deuterium ion implantation, an additional peak corresponding to the deuterium content occurs at about 600–1200 nm. This is the deposition area of the incident deuterium ion. In comparison with the Stopping and Range of Ions in Matter (SRIM) results (Fig. 5), the additional peak position of deuterium content is similar to the deposition peak calculated by SRIM. However, the additional peak is slightly broadened due to deuterium diffusion from high concentration area to low concentration area in the film. As seen in the Fig. 4, the broadening is greater at the surface of the film. This phenomenon is probably due to the dependency of diffusion rate on the temperature. Forced water cooling on the back end of the target weakens the diffusion of deuterium into the film. The surface thermal effect of the film is more obvious to promote the diffusion of deuterium to the surface.

With the increase of the deuterium ion implantation, the deuterium accumulation in the deposition region and the deuterium diffusion are more obvious. Surprisingly the deuterium content of the film surface decreases with the increase of the number of implanted ion. We speculate that thermal effects will increase the deuterium equilibrium pressure at the surface, which leads to deuterium desorption of the surface. At the same time, the radiation damage caused by a large number of deuterium ions decreases the migration rate of deuterium in the film.

Sample S3 was stored in a vacuum storage vessel (10^{−3} Pa, 300 K) for two months (called sample S4) and then characterized again. Figure 6 shows the deuterium concentration as a function of depth in the film. Surprisingly,

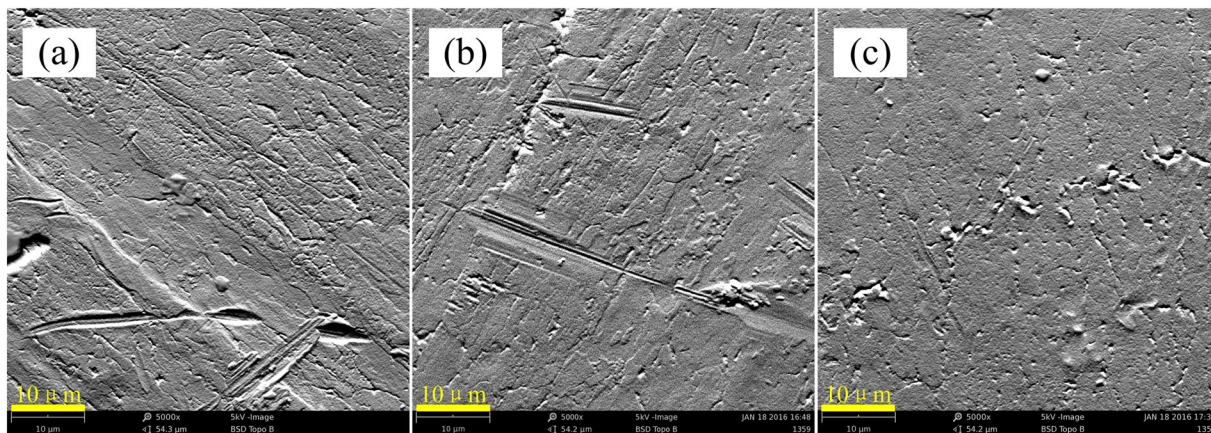


Figure 1. Surface morphologies of the as-grown sample (a) and ion-implanted samples (b,c).

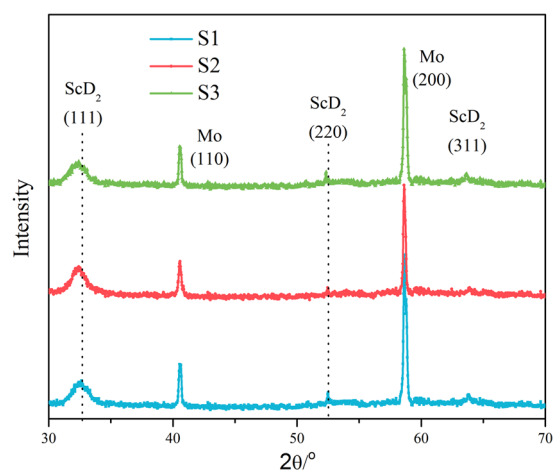


Figure 2. XRD patterns of the scandium deuteride films after irradiation.

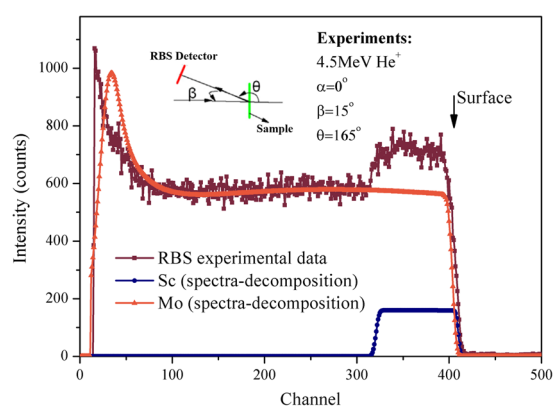


Figure 3. Energy spectrum of He^+ particles scattered from ScD_x/Mo film.

deuterium in the deposition region is fully diffused and the whole film is basically in equilibrium. In contrast to Ar and O, deuterium diffuses rapidly at room temperature. Moreover, the concentration of deuterium is restored to the original value before D-D reaction, implying a self-healing capability. We hypothesize that this is due to the fact that the defects have a stronger pinning effect on the deuterium atom, which is much more important than the diffusion effect based on the chemical potential difference^{32–35}. Besides, there is a slight increase in the surface deuterium content. This indicates that the diffusion of deuterium is weakened at the surface area. Compared to sample S1, the deuterium contents of S3 and S4 decrease significantly at the surface of the film.

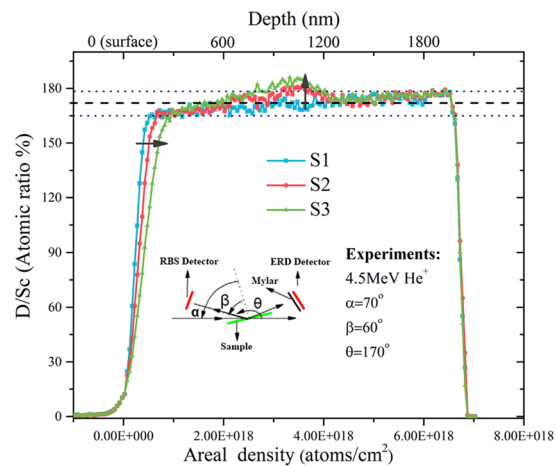


Figure 4. Deuterium concentration of S1, S2 and S3 with different depth in the film.

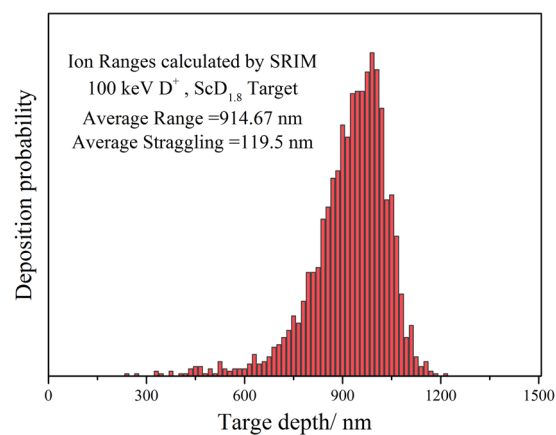


Figure 5. Deuterium deposition peak calculated by SRIM results.

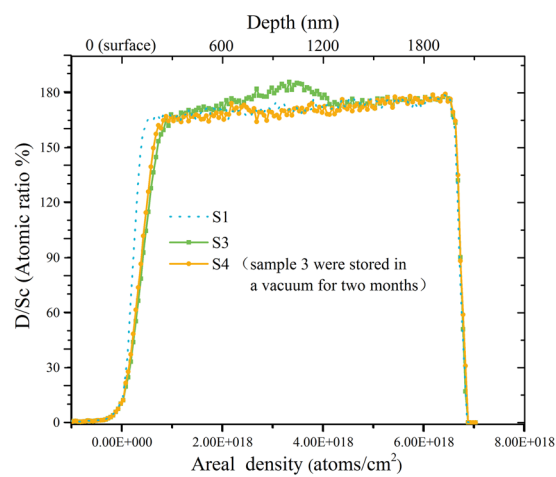


Figure 6. Deuterium concentration of S1, S3 and S4 with different depth in the film.

Conclusions

We have carried out SEM, XRD, RBS and ERDA studies of the diffusion and distribution of deuterium in ScD_x/Mo thin films before and after irradiation of deuterium ions. With the increase of the deuterium ion implantation, the deuterium accumulation in the deposition region and the deuterium diffusion is more obvious. It is found that deuterium diffuses rapidly at room temperature and the concentration of deuterium at the implanted region returns to the original state. Such a self-healing effect is of great importance for the long-term stability of neutron generators based on D-D reaction.

References

- Reijonen, J. Neutron generators developed at LBNL for homeland security and imaging applications. *Nucl. Instr. and Meth. Phys. Res. B* **261**, 272–276 (2007).
- Chakoumakos, B. C., Pracheil, B. M., Koenigs, R. P., Bruch, R. M. & Feygenson, M. Empirically testing vaterite structural models using neutron diffraction and thermal analysis. *Sci. Rep.* **6**, 36799 (2016).
- Tremis, A. S., Rakovan, J., Shinohara, T., Kockelmann, W., Losko, A. S. & Voge, S. C. Non-destructive study of bulk crystallinity and elemental composition of natural gold single crystal samples by energy-resolved neutron imaging. *Sci. Rep.* **7**, 40759 (2017).
- Zhang, W., Bodey, A. J., Sui, T., Kockelmann, W., Rau, C., Korsunsky, A. M. & Mi, J. Multi-scale characterisation of the 3D microstructure of a thermally-shocked bulk metallic glass matrix composite. *Sci. Rep.* **6**, 18545 (2016).
- Wambersie, A., Richard, F. & Breteau, N. Development of fast-neutron therapy worldwide-radiobiological, clinical and technical aspects full source. *Acta-Oncologica-Stockholm* **33**, 216–274 (1994).
- Loeper, B., Wagner, F. M., Budel, S., Harfensteller, M., Voit, A. & Henkelmann, R. Neutrons for medicine. *Neutron News* **21**, 16–19 (2010).
- Koizumi, C. J. Neutron capture logging calibration and data analysis for environmental contaminant assessment. *Journal of Applied Geophysics* **61**, 111–131 (2007).
- Frankle, C. M. & Dale, G. E. Unconventional neutron sources for oil well logging. *Nucl. Instr. and Meth. Phys. Res. A* **723**, 24–29 (2013).
- Kim, L. J., Jung, N. S., Jung, H. D., Hwang, Y. S. & Choi, H. D. A D-D neutron generator using a titanium drive-in target. *Nucl. Instr. and Meth. Phys. Res. B* **266**, 829–833 (2008).
- Yamawaki, M., Suwarno, H., Yamamoto, T., Sanda, T., Fujimura, K., Kawashima, K. & Konashi, K. Concept of hydride fuel target subassemblies in a fast reactor core for effective transmutation of MA. *J. Alloy. Comp.* **530**, 271–273 (1998).
- Wojciech, L., Enrico, G., Zbigniew, K. & Mark, A. S. Decomposition of thin titanium deuteride films thermal desorption kinetics combined with microstructure analysis. *Appl. Surf. Sci.* **254**, 2629–2637 (2008).
- Monnin, C., Ballanger, A., Sciora, E., Steinbrunn, A., Alexandre, P. & Pelcot, G. Characterization of deuteride titanium targets used in neutron generators. *Nucl. Instr. and Meth. Phys. Res. A* **453**, 493–500 (2000).
- Bystritsky, V. M., Dudkin, G. N., Filipowicz, M., Z. h, T. Y. & Zhakanbaev, E. A. Targets of deuterides TiD₂, ZrD₂, NbD₂ and CrD₂ with different structures used in experiments on the study of pd and d-d reactions at astrophysical energies. *Nucl. Instr. and Meth. Phys. Res. A* **810**, 80–85 (2016).
- Liu, Y., Xiang, W., Zhang, G. & Wang, B. Surface and phase transformation characteristics of titanium hydride film under irradiation of pulsed ion beam. *Appl. Surf. Sci.* **285P**, 557–563 (2013).
- Wang, B., Liu, Y., Qin, X. & Xiang, W. A comparative study between pure titanium and titanium deuteride targets used for neutron generator. *Surface and Coatings Technology* **228**, 142–145 (2013).
- Carole, M., Pierre, B., Pierre, A. T., Marc van, R. & Anne, B. Optimization of the manufacturing process of tritide and deuteride targets used for neutron production. *Nucl. Instr. and Meth. Phys. Res. A* **480**, 214–222 (2002).
- Wu, Q., Bing, W., Long, X., Zhou, X., Liu, J. & Luo, S. Thermodynamics and kinetics of deuterium absorption in scandium system. *J. Fusion Energy* **32**, 56–61 (2013).
- David, P. A., Laurence, E. B., Ronald, G., Juan, A. R., & Beverly, S. Evolution of stress in ScD₂/Cr thin films fabricated by evaporation and high temperature reaction. *Sandia Report SAND2001-1629* (2001).
- David, P. A., Juan, A. R., Mark, A. R., Jerry, A. F., & Paul, G. K. Microstructures, phase formation, and stress of reactively deposited metal hydride thin films. *Sandia Report SAND2002-1466* (2002).
- Lundin, C. E. The structural and thermodynamic properties of the Sc-H system. *Sandia Report SAND72-3158* (1972).
- Manchester, F. D. & Pitre, J. M. The H-Sc (Hydrogen-Scandium) system. *J. Phase Equilibria* **18**, 194–204 (1997).
- Verbeke, J. M., Leung, K. N. & Vujic, J. Development of a sealed-accelerator-tube neutron generator. *Appl. Radiat. Isotopes* **53**(4–5), 801–809 (2000).
- Ye, X. Q., Tang, T., Ao, B. Y., Luo, D. L., Sang, G. & Zhu, H. Z. Thermodynamics of Sc-H and Sc-D system: experimental and theoretical studies. *J. Fusion Energy* **32**, 254–257 (2013).
- Le-Quoc, H., Lacoste, A., Miraglia, S., Bechu, S., Bes, A. & Laversenne, L. MgH₂ thin films deposited by one-step reactive plasma sputtering. *Int. J. Hydrogen Energy* **39**, 17718–17725 (2014).
- Platzer-Bjorkman, C., Mongstad, T., Mahlen, J. P., Baldi, A., Karazhanov, S. & Holt, A. Transparent yttrium hydride thin films prepared by reactive sputtering. *Thin Solid Films* **519**, 5949–5954 (2011).
- Weib, V., Seeger, S., Ellmer, K. & Mientus, R. Reactive magnetron sputtering of tungsten disulfide (WS_{2-x}) films: Influence of deposition parameters on texture, microstructure, and stoichiometry. *J. Applied Physics* **101**, 103502 (2007).
- Schiettekatte, F. & Ross, G. G. ErD spectrum to depth profile conversion program for windows. *AIP Conf. Proc.* **392**, 711–714 (1996).
- Mayer M. SIMNRA, Max-Planck-Institut für Plasmaphysik, Garching, Version 6.03.
- Tsuchiya, B. et al. Hydrogen analyses of titanium hydride by ERD and NRGmethods. *Nucl. Instr. and Meth. Phys. Res. B* **190**, 699–703 (2002).
- Kennedy, J., Markwitz, A., Trodahl, H. J., Ruck, B. J., Durbin, S. M. & Gao, W. Ion beam analysis of amorphous and nanocrystalline group III-V nitride and ZnO thin films. *J. Electronic Materials* **36**(4), 472–482 (2007).
- Kennedy, V. J., Markwitz, A., Lanke, U. D., McIvor, A., Trodahl, H. J. & Bittar, A. Ion beam analysis of ion-assisted deposited amorphousGaN. *Nucl. Instr. and Meth. Phys. Res. B* **190**, 620–624 (2002).
- Scully, J. R., Young, G. A. Jr. & Smith, S. W. Hydrogen solubility, diffusion and trapping in high purity aluminum and selected Al-base alloys. *Materials Science Forum* **331–337**, 1583–1600 (2000).
- Fukai, Y. & Sugimoto, H. Formation mechanism of defect metal hydrides containing superabundant vacancies. *J. Phys. Condens. Matter* **19**, 436201 (2007).
- Xie, D. G. et al. Hydrogenated vacancies lock dislocations in aluminum. *Nature Communications* **11**, 13341 (2016).
- Li, S. Z. et al. The interaction of dislocations and hydrogen-vacancy complexes and its importance for deformation-induced protonano-voids formation in a-Fe. *International Journal of Plasticity* **74**, 175–191 (2015).

Acknowledgements

X.R.W. acknowledges supporting of Elite Nanyang Professorship from Nanyang Technological University, Singapore.

Author Contributions

Tao Wang, Jidong Long and Linwen Zhang designed the study; Gang Huang washed the molybdenum substrates; Tao Wang and Shiwei Wang prepared samples of ScDx films; Tao Wang, Zhen Yang and Jie Li carried out ion irradiation experiments; Tao Wang carried out other characterization experiments (SEM, XRD, RBS, ERDA); Tao Wang, Jidong Long and Xiao Renshaw Wang collected the data and performed the refinements; Tao Wang, Allen Jian Yang and Xiao Renshaw Wang wrote the paper; all authors contributed to the final paper.

Additional Information

Competing Interests: The authors declare that they have no competing interests.

Publisher's note: Springer Nature remains neutral with regard to jurisdictional claims in published maps and institutional affiliations.



Open Access This article is licensed under a Creative Commons Attribution 4.0 International License, which permits use, sharing, adaptation, distribution and reproduction in any medium or format, as long as you give appropriate credit to the original author(s) and the source, provide a link to the Creative Commons license, and indicate if changes were made. The images or other third party material in this article are included in the article's Creative Commons license, unless indicated otherwise in a credit line to the material. If material is not included in the article's Creative Commons license and your intended use is not permitted by statutory regulation or exceeds the permitted use, you will need to obtain permission directly from the copyright holder. To view a copy of this license, visit <http://creativecommons.org/licenses/by/4.0/>.

© The Author(s) 2017